

Multifunctional Nanoscale Platform for the Study of T Cell Receptor Segregation

Esti Toledo, Muhammed Iraqi, Ashish Pandey, Sivan Tzadka, Guillaume Le Saux, Angel Porgador, and Mark Schwartzman*



Cite This: *ACS Omega* 2023, 8, 28968–28975



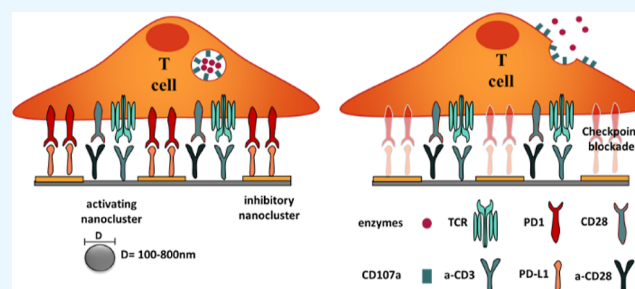
Read Online

ACCESS |

Metrics & More

Article Recommendations

ABSTRACT: T cells respond not only to biochemical stimuli transmitted through their activating, costimulatory, and inhibitory receptors but also to biophysical aspects of their environment, including the receptors' spatial arrangement. While these receptors form nanoclusters that can either colocalize or segregate, the roles of these colocalization and segregation remain unclear. Deciphering these roles requires a nanoscale platform with independent and simultaneous spatial control of multiple types of receptors. Herein, using a straightforward and modular fabrication process, we engineered a tunable nanoscale chip used as a platform for T cell stimulation, allowing spatial control over the clustering and segregation of activating, costimulatory, and inhibitory receptors. Using this platform, we showed that, upon blocked inhibition, cells became sensitive to changes in the nanoscale ligand configuration. The nanofabrication methodology described here opens a pathway to numerous studies, which will produce an important insight into the molecular mechanism of T cell activation. This insight is essential for the fundamental understanding of our immune system as well as for the rational design of future immunotherapies.



INTRODUCTION

T cell function is regulated by activating and costimulatory receptors, whose binding to the ligands expressed by target cells initiates signaling cascades that determine the T cell immune response.^{1,2} To maintain the balance between self-tolerance and autoimmunity of our immune system, the activating and costimulatory signaling is suppressed by inhibitory receptors, which are also called inhibitory checkpoints. The two most studied inhibitory receptors are cytotoxic T-lymphocyte-associated protein 4 (CTLA-4) and programmed death receptor 1 (PD-1), which are, in particular, expressed by tumor cells to evade the immune surveillance of T cells. In recent years, blockade of CTLA-4 and PD-1 with their antibodies has emerged as a revolutionary treatment for several types of cancer.^{3–5}

The function of immune checkpoints has been extensively studied since its discovery. While the biochemical aspects of PD-1 activity are well reported, such as PD-1-mediated phosphatase recruitment,⁶ the ensuing deactivation of T cell (TCR),⁷ and costimulatory (CD28) receptor signaling,⁸ much less is known of the physical aspects of the inhibitory signaling mechanism. For example, it is known that T cell activating, costimulatory, and inhibitory receptors are organized into highly regulated nanoscale clusters, which segregate or colocalize at different stages of T cell activation.^{9–11} However,

the effect of receptor clustering and segregation on the integration of activating and inhibitory signals is still unclear. In light of the fact that inhibitory receptors must colocalize with activating receptors to suppress the signaling of the latter,¹² deciphering the exact role of receptor colocalization or segregation on inhibitory signaling requires a platform on which distinct receptors can be spatially controlled and the ensuing response of T cells can be monitored.

Recent advances in nanotechnology have allowed the engineering of cell-stimulating surfaces coated with controlled molecular patterns of ligands, which, in turn, determine receptor arrangement within the cell membrane at the nanometric scale.^{13–16} In the context of immune receptors, nanopatterns of activating ligands for T cells and for natural killer (NK) cells were recently used to study the effect of receptor spatial arrangement on the motility and immune response of these cells.^{17–22} Alternatively, the distribution of T cell receptors can be controlled by patterns realized using DNA

Received: January 18, 2023

Accepted: May 10, 2023

Published: August 1, 2023



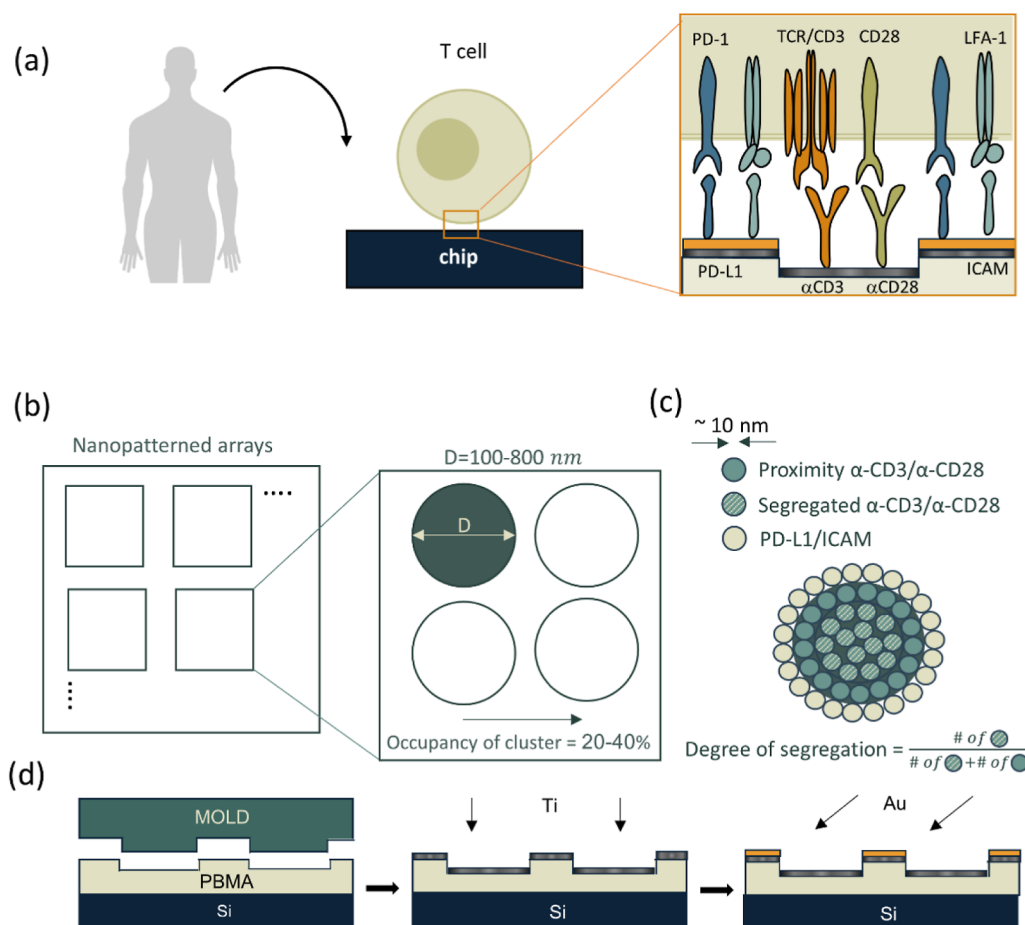


Figure 1. Schematic representation, chip design, and fabrication of the nanochip for the control of segregation of T cells. (a) Schematic representation of the chip and spatial organization of ligands on the chip surface. (b) Chip design with cluster size and density. (c) Schematic representation of ligand patterns. Colocalized or spatially segregated ligands control the spatial arrangement of integrating receptors. (d) Chip fabrication process flow showing nanoimprint lithography using a hybrid mold on a silicon substrate coated with thermal resist. Straight evaporation of titanium and angle evaporation of gold. The human silhouette was taken from [VectorStock.com](https://www.vectorstock.com) and is a free domain.

origami.^{23,24} However, these nanopatterns could only position the activating/costimulatory receptor. Therefore, such nanopatterns could not be used to study how the arrangement of different receptors, i.e., activating and inhibitory ones, affects their signaling integration. Recently, we demonstrated a novel approach for nanofabricated molecular-scale patterns of controllably positioned activating and inhibitory ligands for NK cells and used this approach to elucidate the effect of spacing between the activating and inhibitory receptors on the inhibition in NK cells.²⁵ However, because these patterns controllably positioned single activating and inhibitory ligands, they did not mimic the nanoscale clustering of activating and inhibitory ligand–receptor constructs at the interface between the lymphocyte (e.g., T cell or NK cell) and its target. Studying receptor segregation requires nanofabrication approaches that allow for the configuration of activating and inhibitory receptors into controlled nanoscale clusters.

Here, we engineered a tunable nanoscale chip used as a platform for T cell stimulation, allowing spatial control over the clustering and segregation of activating, costimulatory, and inhibitory receptors. Specifically, we designed the chip surface with arrays of patterned discoid nanoclusters filled with homogeneously mixed antibodies for CD3 ζ and CD28. These antibodies engage TCR and CD28, respectively, whose colocalization within nanoscale clusters produces

optimal activating–costimulatory signaling essential for T cell activation.²⁶ Furthermore, to introduce spatially segregated inhibitory cues, the background of the clusters was patterned with PD-L1—a ligand for PD-1 (Figure 1a).

We designed a nanochip containing various nanoclusters with controllably varied sizes and distribution. Each array was $400 \mu\text{m}$ in size. The diameter of the clusters in the arrays ranged between 100 and 800 nm, which corresponds to the size scale of the nanometric receptor clusters microscopically on the interface between T cells and their target.¹¹ Also, we used two types of arrays, in which the overall surface coverage of the clusters was 20 and 40% (Figure 1b). In that way, we defined not only the relative positions of the activating, costimulatory, and inhibitory ligands but also their “degree of segregation”. Indeed, for an array of discoid clusters of activating/costimulatory ligands, only those lying at the disk periphery are in close contact with the inhibitory ligands and are thus considered as “proximal” ligands. Based on recent reports on the colocalization between the inhibitory and activating or costimulatory nanoclusters,^{6,8} it can be hypothesized that the effective inhibitory signaling requires close proximity between the inhibitory and/or costimulatory receptors. In the context of our chip design, it means that the signaling produced by TCR and CD28 bound to these proximal ligands is expected to be mostly prone to inhibition

by PD-1 receptors attached to the cluster periphery. Inversely, other ligands within the cluster, which are positioned away from the cluster periphery, can be considered as “segregated ligands” since they are not in direct contact with the inhibitory ligands that are on the background. According to the same hypothesis, these segregated ligands are less prone to inhibition. The relative amount of the segregated ligands among all the ligands within the cluster is determined here as the degree of segregation. The degree of segregation can be calculated for each cluster size, taking into account that the footprint of individual activating and inhibitory ligands is about 100 sq nm^{20,27–29} and assuming that the ligands are immobilized onto the chip surface in a closely packed configuration (details of calculations are given in the experimental section). Also, control surfaces were fabricated, in which all the ligands were homogeneously mixed. Overall, on the stimulation platforms used here, including the control chips, the degree of segregation ranged from 0.76 to 0.96 (Figure 1c).

The chip was fabricated by a novel approach based on nanoimprint lithography and angle evaporations, which resulted in bimetallic patterns of Au nano-islands surrounded by an oxidized Ti background, with no need for pattern transfer by etching of liftoff. This pattern was biofunctionalized in a site-selective manner using (i) Au–thiol and (ii) TiO₂–silane PEG biotin avidin and nitrilotriacetic acid (NTA)–Ni–histidine conjugations respectively.³⁰ To improve the adhesion of T cells to the chip surfaces, PD-L1 was diluted with an intercellular adhesion molecule (ICAM). We verified the site selectivity of this orthogonal functionalization, which is critical for the chip fabrication, using fluorescence microscopy. As proof of concept, we used this multifunctional nanoscale platform to examine how ligand clustering and segregation affected cytotoxic T cell activity. Furthermore, we examined how the spatially controlled inhibition of T cell activation is reduced by the immune checkpoint blockade. In summary, our platform allows for the independent control of three crucial variables that determine cell behavior: ligand density, clustering, and segregation, and the modularity of our approach will expedite the advent of future studies of the structure and mechanism of functional biointerfaces in multiple applications.

MATERIALS AND METHODS

Platform Design and Fabrication. The chip was fabricated by producing arrays of nanoscale disks of oxidized titanium on a gold background using nanoimprint lithography and site-selective functionalization of the two metals with the ligands. First, a master mold was produced by electron beam lithography and plasma etching. The mold surface contained arrays of etched nanoscale pits with variable diameters, which corresponded to the designed cluster size. The depth of the pits was about 100 nm. The nanopattern was then transferred from the master mold to a soft nanoimprint mold,³¹ which was then used to thermally imprint a thin film of resist (polybenzyl methacrylate, PBMA) on silicon.³² The imprint process was then done with a nanoimprint tool (NX-B100, Nanonex) with the following parameters: pressure of 100 psi and temperature of 100 °C for 5 min. 10 nm titanium was evaporated followed by 10 nm of gold at an angle of 80°. The imprint was followed by two sequential metal evaporations: straight evaporation of 5 nm of Ti and angle evaporation (85°) of 10 nm of Au. Here, the shadowing effect produced by the pit topography ensured

that only the area outside the circles was covered by gold, while titanium covered the inner circle area (Figure 1d). It must be noted that after exposing the chip to air, the surface of titanium spontaneously oxidizes.

The degree of segregation was calculated as follows: first, the area of the outer ring with a 10 nm width was subtracted from the cluster area. This area corresponds to the ring of activating and costimulatory antibodies which are in contact with the inhibitory PD-1 ligands. The remaining portion of the cluster corresponds to the area occupied by activating and costimulatory antibodies, which are segregated from the inhibitory ligands. Then, this area was divided by the total cluster area to give the degree of segregation (Figure 1c).

Selective Biofunctionalization of the Platform. An orthogonal approach was used to selectively immobilize the ligands onto titanium circles and gold background.³⁰ First, oxidizing titanium was functionalized. The samples were cleaned in plasma cleaning for 1 min and were immersed in a 20 μM ethanolic solution of silane PEG Biotin for 24 h. The samples were placed in an oven at 60 °C for 4 h without rinsing. The samples were then copiously rinsed with water and ethanol. Au was functionalized by reacting overnight in a 0.2 mM ethanolic solution of thiol–NTA. After generous rinsing with ethanol and water, the samples were blocked for 30 min at 37 °C in PBS with 5% BSA, followed by 30 min of incubation in 25 μg/mL NeutrAvidin Oregon Green 488 in PBS with 5% BSA at room temperature. The surfaces were rinsed in PBS with 0.1% Tween 20. The samples were then incubated for 2 h in nickel(II) chloride, followed by rinsing in water. The samples were then incubated overnight at 4 °C in 2 μg/mL of histidine-tagged PD-L1 and ICAM (1:1). Then, the samples were incubated overnight at 4 °C in 2 μg/mL of biotinylated anti-CD3 (OKT3) and CD28 (1:1). Finally, the samples were rinsed in PBS with 0.1% Tween 20 plus once with neat PBS and stored in PBS before being used for cell studies. To verify the biofunctionalization selectivity, allophycocyanin (APC)-tagged goat anti-rabbit IgG was attached to the ligand PD-L1 via rabbit anti-human PD-L1. Also the biotinylated OKT3 was attached to the Oregon Green 488-tagged NeutrAvidin, and Alexa Fluor 568-labeled goat anti-mouse IgG was attached to the OKT3.

Isolating and Culturing of the Human CD8+ T Cells. Peripheral blood mononuclear cells (PBMCs) were isolated from blood obtained from a healthy donor using the FICOLL gradient.^{33,34} First, blood was diluted in 2% fetal bovine serum in a 1:1 ratio and then loaded on 10 mL of FICOLL gradient in 50 mL centrifuge vials and centrifuged at 287 g-force [1200 rounds per minute (rpm) in a centrifuge (Eppendorf, 5810R) with 17.8 cm diameter] with no forced breaks or acceleration. The collected PBMCs (buffy coat) were cultured in complete RPMI media, supplemented with 10% human serum, 200 U/mL of IL-2, and 50 ng/mL of OKT-3 for 2 days. Isolation of the CD8+ T cells was performed with a positive selection of CD8+ beads (130-045-201, Macs Miltenyi Biotec) using a magnetic column according to the manufacturer’s instructions. CD8+ T cells were continuously cultured in complete RPMI media, supplemented with 10% human serum and 200 U/mL of IL-2 only.

Cell Study. Cultured T-cells (5×10^5 /mL, cultured as detailed below) were seeded onto αα-CD3-functionalized platform in a complete RPMI media containing <10% human serum (Male AB, H4522) and 200 units of IL-2 (200-02-500UG, Peprotech). For the imaging of CD107a, a

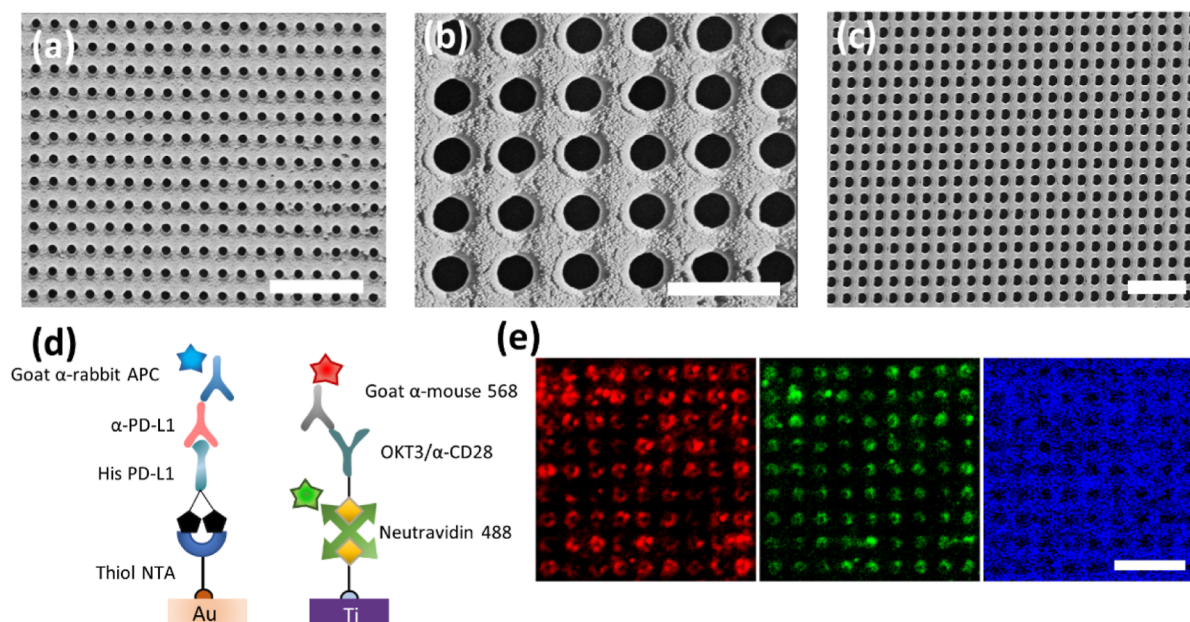


Figure 2. Results of fabrication and biofunctionalization. (a–c) SEM images of nanoclusters in different fields with various sizes of 200, 300, and 800 nm, respectively. Scale bar left to right: 5, 1, and 5 μm . (d) Schematic process of the functionalization of oxidized titanium and the gold surface. (e) Fluorescent images of a functionalized array made of oxidized titanium and background of gold taken in the red channel, green channel, and blue channel, respectively. Scale bar: 5 μm .

degranulation marker, the medium was supplemented with APC anti-human CD107a antibodies (1:1000 v/v, 328,620, BioLegend) and was left to adhere for 3 h. After 3 h of incubation, samples were rinsed twice in PBS to remove the nonadherent cells, and cells were fixed with 4% paraformaldehyde (PFA) at 4 $^{\circ}\text{C}$ for 10 min. The PFA was then replaced with PBS, and the samples were rinsed once with PBS. The actin cytoskeleton was stained with Alexa Fluor 555 phalloidin (1:40) (Life Technologies) in PBS with 5% skim milk by incubating at 37 $^{\circ}\text{C}$ for 1 h. Importantly, cells were not permeabilized to maintain membrane integrity and thus allow for imaging of membrane-bound anti-CD107a. The samples were finally rinsed once with PBS and once with distilled water. The nuclei were stained by mounting the samples with ProLong Gold antifade reagent containing DAPI (Life Technologies). Samples were imaged using a Nikon Ti2e epifluorescence microscope and analyzed using Fiji software. High-resolution cell imaging was performed by acquiring images using a Zeiss LSM 880 confocal microscope.

Statistics. All biological experiments were performed three times. 30 to 60 regions were imaged and averaged for quantification. Statistical analysis was performed by analysis of variance, and Tukey's multiple comparison post hoc test was also performed. The results were considered to be significantly different for $P < 0.05$.

RESULTS AND DISCUSSION

Effective fabrication of the nanoarrays was demonstrated by SEM, showing discs of titanium surrounded by gold (Figure 2a–c). The site-selectivity of the functionalization was verified using confocal fluorescent microscopy (Figure 2d,e). To that end, the immobilized PD-L1 was immunostained with α -PD-L1, followed by the attachment of APC-tagged secondary antibody (blue). Concurrently, the used NeutrAvidin was tagged with Oregon Green 488 (green). Finally, the immobilized anti-CD3 was stained with the Alexa-fluor 568-

tagged secondary antibody (red). Figure 2e shows the same array imaged in red, green, and blue channels. It can be seen that the patterns produced by the three colors precisely match the array geometry, confirming that the used orthogonal functionalization is highly site-specific and allows a clear separation between the ligands on the chip array.

The nanofabricated arrays of ligands can be used as surrogate microenvironments for the controlled stimulation of T cells.^{6,8} To demonstrate such a study, primary CD8+ T cells were isolated from the peripheral blood of a healthy adult donor, stimulated on the chip surface for 3 h, and fixed. The immune response of T cells was assessed through the membrane immobilization of lysosome-associated membrane protein-1 (CD107a),²⁸ which is a broadly used marker for the degranulation of T cells.³⁵ For this purpose, a fluorescently tagged antibody for CD107a was added to the incubation medium during the stimulation, and its intensity was quantified by fluorescent imaging. Figure 3a,b presents representative images of T cells stimulated on patterns with different densities and cluster sizes, which express different amounts of CD107a (Figure 3c,d). The cells were stained with phalloidin for the cytoskeleton and with DAPI for nuclei to facilitate their imaging. The obtained signals were normalized to the average CD107a expression on a negative control surface, which included a continuous, closely packed film of PD-L1 and ICAM. It can be seen that T cells on all the tested arrays expressed a similarly low amount of CD107a regardless of cluster size. One possible explanation for this low level of activation is that the inhibitory signaling of the PD1 engaged by the PD-L1 out of the nanoclusters is strong enough to suppress any activating and costimulatory signaling produced by TCR and CD-28 despite the fact that most of their cognate antibodies are spatially segregated from PD-1. Surprisingly, this suppression of activation was observed even for arrays where most of the inhibitory and activating ligands were positioned with a high degree of segregation. On the other hand, control

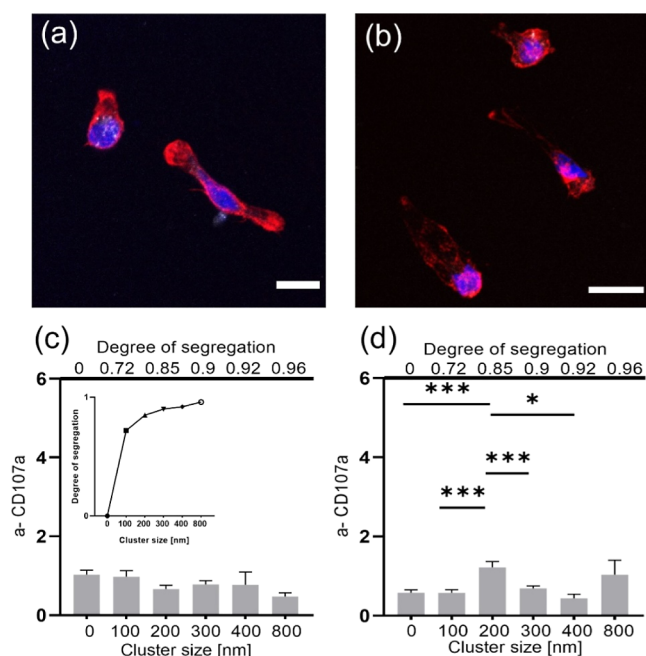


Figure 3. T cells activation. (a) Fluorescent imaging of activation expression on the surface with 0 segregation. (b) Fluorescent imaging of activation expression on the surface with 0.96 segregation. The cells were stained with phalloidin for the cytoskeleton (red), DAPI for the nucleus (blue), and anti-CD107a (white). (c,d) Normalized amount of bound α -CD107a per cell on ligand patterns compared to that of cells stimulated on a surface with mixed ligands. All the data normalized to the control surface with only inhibitory ligands. (c) 20% of activating ligands. (d) 40% of activating ligands. The small graph in (c) shows the degree of segregation against cluster size.

surfaces with zero degrees of segregation produced the same low activation of T cells as the arrays of the cluster did.

To test whether and how the low activation of T cells stimulated on the arrays of anti-CD3/antiCD28 nanoclusters was affected by the engagement of PD-1 outside the clusters, we carried out a control experiment, in which we stimulated T cells on the chip in the presence of its commercial PD-1 antibody pembrolizumab (Keytruda) (Figure 4a). Pembrolizumab is used as an immunotherapeutic drug against several types of cancers due to its ability to effectively block PD-1 in T cells, thereby increasing T cells' antitumor activity. Figure 4b,c presents the average α -CD107a signals per cell for T cells stimulated on the chip in the presence of pembrolizumab. In contrast to T cell stimulation without the PD-1 blockade, in which the ligand configuration in nanoclusters had a negligible effect on the immune response, pembrolizumab-treated T cells produced a highly dependent response to the ligand configuration (Figure 4c,d). For a homogenous mix of ligands (zero degrees of segregation), the pembrolizumab treatment seemed to abrogate the PD-1-based inhibition, resulting in a relatively high CD107a expression. This abrogation, however, became lower for ligands configured into small 100 nm clusters that corresponded to the low segregation of 0.72 and vanished for most of the arrays with larger clusters and higher degrees of segregation. To emphasize the effect of pembrolizumab treatment and its dependence on the ligand configuration in clusters, Figure 4e,f shows the fold change in the CD107a signal between T cells stimulated without and with pembrolizumab. The data further confirm that pembrolizumab

treatment was effective mostly for zero or very small degrees of segregation.

The results of the control experiment confirm that the activation of T cells stimulated without pembrolizumab treatment (Figure 4) was suppressed by the inhibitory effect of PD-L1 immobilized on the cluster background. However, this effect was pronounced only for surfaces with zero or small degrees of segregation. On the contrary, the clusters larger than 100 nm produced an insufficient activation of T cells with and without pembrolizumab treatment. This insufficient activation could probably stem from the cluster geometry and configuration, which presumably were not optimal for T cell activation. Indeed, the clustering of TCR is a critical factor in the regulation of T cell activation. Still, whether and how the mixture of activating antibodies confined into the nanoclusters of variable size determine TCR clustering remain unclear, and addressing this question requires further studies. These studies should include monitoring of both the early signaling in T cells, using markers such as TCR phosphorylation,¹⁰ as well as T cell cytotoxicity, which can be quantified through the release of cytokines such as interferon-gamma.³⁶

This work demonstrates a robust approach for producing a stimulation platform for T cells with a nanoscale control over the clustering and segregation of multiple ligands with antagonist functionalities. At the base of this platform is a bi-metallic nanopattern, which is fabricated using a high-throughput nanoimprint lithography. Furthermore, the pattern transfer is done using a non-standard approach. Indeed, unlike the usual procedure which consists of, for example, resist etching, metal deposition, and liftoff, we performed two sequential metal depositions, one of them being done at a shadowing angle, thus alleviating the need for plasma etching.

It must be noted that the plasma etching rate is highly affected by the micro-loading effect. Therefore, while producing arrays with various geometries on the same substrate using a pattern transfer process that involves plasma etching of the imprinted resist, the etching rate would vary among differently sized clusters. This could likely result in incomplete pattern transfer for clusters of a specific range of size and pattern distortion due to high over-etch for clusters of another range of sizes. On the other hand, plasma etching is avoided in the pattern transfer approach demonstrated here. Accordingly, the overall process flow is largely simplified, and the pattern transfer fidelity is improved.

The nanofabricated heterogeneous bi-metallic pattern of segregated Au/Ti nanodomains was functionalized using an orthogonal approach that was first demonstrated by us in the fabrication of micron-scale patterns of spatially segregated activating and inhibitory ligands for NK cells,³⁰ yet its downscaling to sub-micron scale has not been shown so far. Importantly, this approach is based on broadly used bioconjugation techniques, making this a versatile approach to orthogonally immobilize any combination of biomolecules on the surface. Here, we demonstrated this by applying it to the combination of activating/costimulatory and inhibitory functionalities for T cells. Furthermore, the site-selectivity of this orthogonal approach was previously demonstrated by fluorescent imaging of (i) a ligand immobilized onto Au through NTA–Ni conjugation and (ii) NeutrAvidin immobilized onto Ti through biotin–NeutrAvidin conjugation. Attachment of NeutrAvidin is an intermediate step in the functionalization process. On the other hand, the site-selective surface immobilization of the second, biotinylated ligand,

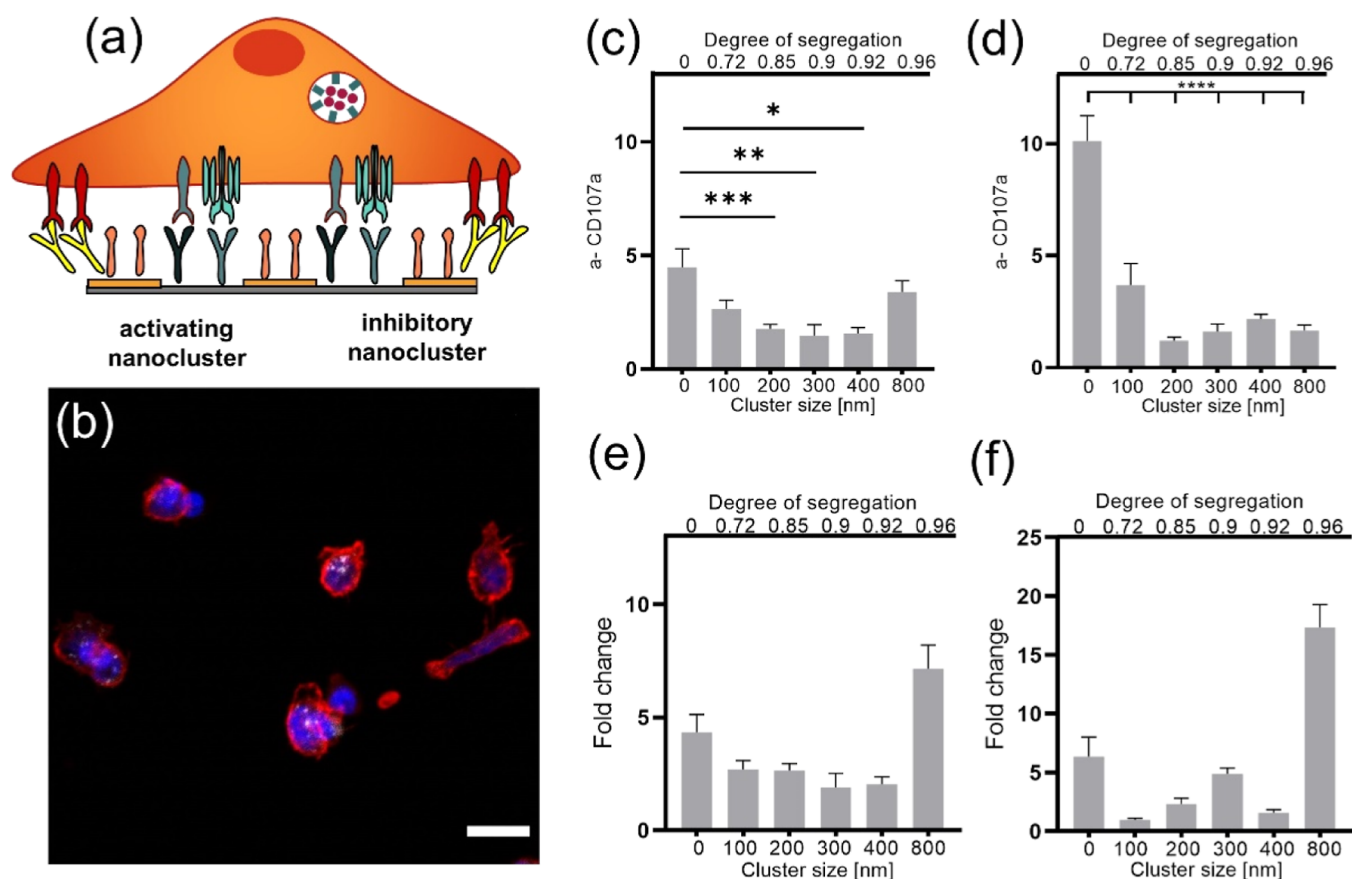


Figure 4. T cell activation with drugs. (a) Schematic representation of T cells on a chip with an inhibitory checkpoint blockade. Fluorescent imaging of activation expression on the surface with maximum proximity. (b) Fluorescent imaging of activation expression of T cells with drugs on the surface with 0.96 segregation. The cells were stained with phalloidin for the cytoskeleton (red), DAPI for the nucleus (blue), and anti-CD107a (white). (c,d) Fold change of α -CD107a according to negative control of only inhibitory ligands. (c) 20% of activating ligands. (d) 40% of activating ligands. (e,f) Fold change of activation between the surface with drugs and without. (e) 20% of activating ligands. (f) 40% of activating ligands.

which is the final step in the functionalization process, was only indirectly verified using a biotin-labeled fluorophore. Here, for the first time, to the best of our knowledge, we confirmed the complete site-selectivity of our orthogonal approach through its final step by separate immunostaining of activating/inhibitory antibodies and PD-L1 and verifying that the produced two-color fluorescent pattern matches the geometry of the fabricated nanoarray.

Micropatterns of segregated functionalities are an emerging tool to study the spatial segregation of different molecules within the cell membrane and their functional cross-talk. Early examples of such micropatterns were fabricated by photolithography combined with orthogonal functionalization. Since then, such patterns have been used to elucidate the effect of chemical heterogeneity of the extracellular environment on vital cell functions, such as motility, proliferation, and differentiation.^{37,38} In the context of the immune function, heterogeneous micropatterns consisting on microdomains of activating ligands surrounded with adhesion ligands were produced by photolithography and used to mimic the geometry of the immunological synapse.³⁹ Another example includes a micropattern of alternating strips of activating and inhibitory antibodies for NK cells produced by contact printing.⁴⁰ Still, all the patterns could allow the spatial segregation between different biomolecules on the micron scale due to the resolution limitations of the used lithography

methods. However, many processes related to the spatial segregation between different biomolecules in the living systems occur at the nanometric scale. To produce an artificial cell-stimulating environment in which different stimulating biomolecules are segregated at the nanoscale, a patterning method is required, which combines nanometric resolution, high throughput, and pattern arbitrariness. This requirement precludes contact printing with limited resolution, electron beam lithography with low throughput, and self-assembly patterning methods that are limited to produce only periodic patterns with one geometry. Thus, nanoimprint lithography, which addresses all three requirements, is the ultimate choice for fabricating patterns with nanoscale segregation of stimulating biomolecules of different functionalities. Our work provides a clear demonstration of the benefits of using nanoimprint lithography to produce such nanopatterns in combination with orthogonal biofunctionalization. Furthermore, the demonstrated fabrication approach paves the way to endless studies aiming to understand how nanoscale biochemical heterogeneity in the extracellular environment affects the functions of cells.

■ AUTHOR INFORMATION

Corresponding Author

Mark Schvartzman – Department of Materials Engineering, Ben-Gurion University of the Negev, Beer-Sheva 8410501,

Israel; Ilse Katz Institute for Nanoscale Science & Technology, Ben-Gurion University of the Negev, Beer-Sheva 8410501, Israel; orcid.org/0000-0002-5912-525X; Email: marksc@bgu.ac.il

Authors

Esti Toledo – Department of Materials Engineering, Ben-Gurion University of the Negev, Beer-Sheva 8410501, Israel; Ilse Katz Institute for Nanoscale Science & Technology, Ben-Gurion University of the Negev, Beer-Sheva 8410501, Israel; orcid.org/0000-0003-3103-816X

Muhammed Iraqi – The Shraga Segal Department of Microbiology, Immunology, and Genetics, Faculty of Health Science, Ben-Gurion University of the Negev, Beer-Sheva 8410501, Israel

Ashish Pandey – Department of Materials Engineering, Ben-Gurion University of the Negev, Beer-Sheva 8410501, Israel; Ilse Katz Institute for Nanoscale Science & Technology, Ben-Gurion University of the Negev, Beer-Sheva 8410501, Israel

Sivan Tzadka – Department of Materials Engineering, Ben-Gurion University of the Negev, Beer-Sheva 8410501, Israel; Ilse Katz Institute for Nanoscale Science & Technology, Ben-Gurion University of the Negev, Beer-Sheva 8410501, Israel

Guillaume Le Saux – Department of Materials Engineering, Ben-Gurion University of the Negev, Beer-Sheva 8410501, Israel; Ilse Katz Institute for Nanoscale Science & Technology, Ben-Gurion University of the Negev, Beer-Sheva 8410501, Israel; orcid.org/0000-0003-4902-1980

Angel Porgador – The Shraga Segal Department of Microbiology, Immunology, and Genetics, Faculty of Health Science, Ben-Gurion University of the Negev, Beer-Sheva 8410501, Israel

Complete contact information is available at:

<https://pubs.acs.org/10.1021/acsomega.2c08194>

Notes

The authors declare no competing financial interest.

ACKNOWLEDGMENTS

This work was funded by the Multidisciplinary Research Grant—The Faculty of Health Science in Ben-Gurion University of the Negev, Israel Science Foundation, Individual grant # 1401/15, and Israel Science Foundations: F.I.R.S.T. Individual grant # 2058/18. E.T. is supported by the Israel Ministry of Science and Technology, Ariane de Rothschild Women's Doctoral scholarships program for outstanding female Ph.D. students, and Israel Scholarship Education Foundation (ISEF).

REFERENCES

- (1) Batista, F. D.; Dustin, M. L. Cell: Cell Interactions in the Immune System. *Immunol. Rev.* **2013**, *251*, 7–12.
- (2) Bromley, S. K.; Burack, W. R.; Johnson, K. G.; Somersalo, K.; Sims, T. N.; Sumen, C.; Davis, M. M.; Shaw, A. S.; Allen, P. M.; Dustin, M. L. The Immunological Synapse. *Annu. Rev. Immunol.* **2001**, *19*, 375–396.
- (3) Wei, S. C.; Duffy, C. R.; Allison, J. P. Fundamental Mechanisms of Immune Checkpoint Blockade Therapy. *Cancer Discovery* **2018**, *8*, 1069–1086.
- (4) Menon, S.; Shin, S.; Dy, G. Advances in Cancer Immunotherapy in Solid Tumors. *Cancers* **2016**, *8*, 106.
- (5) Rosner, S.; Reuss, J. E.; Forde, P. M. PD-1 Blockade in Early-Stage Lung Cancer. *Annu. Rev. Med.* **2019**, *70*, 425–435.

(6) Yokosuka, T.; Takamatsu, M.; Kobayashi-Imanishi, W.; Hashimoto-Tane, A.; Azuma, M.; Saito, T. Programmed Cell Death 1 Forms Negative Costimulatory Microclusters That Directly Inhibit T Cell Receptor Signaling by Recruiting Phosphatase SHP2. *J. Exp. Med.* **2012**, *209*, 1201.

(7) Riley, J. L. PD-1 Signaling in Primary T Cells. *Immunol. Rev.* **2009**, *229*, 114–125.

(8) Hui, E.; Cheung, J.; Zhu, J.; Su, X.; Taylor, M. J.; Wallweber, H. A.; Sasmal, D. K.; Huang, J.; Kim, J. M.; Mellman, I.; Vale, R. D. T Cell Costimulatory Receptor CD28 Is a Primary Target for PD-1-Mediated Inhibition. *Science* **2017**, *355*, 1428–1433.

(9) Yokosuka, T.; Kobayashi, W.; Takamatsu, M.; Sakata-Sogawa, K.; Zeng, H.; Hashimoto-Tane, A.; Yagita, H.; Tokunaga, M.; Saito, T. Spatiotemporal Basis of CTLA-4 Costimulatory Molecule-Mediated Negative Regulation of T Cell Activation. *Immunity* **2010**, *33*, 326–339.

(10) Pigeon, S. V.; Tabarin, T.; Yamamoto, Y.; Ma, Y.; Nicovich, P. R.; Bridgeman, J. S.; Cohnen, A.; Benzinger, C.; Gao, Y.; Crowther, M. D.; Tungatt, K.; Dolton, G.; Sewell, A. K.; Price, D. A.; Acuto, O.; Parton, R. G.; Gooding, J. J.; Rossy, J.; Rossjohn, J.; et al. Functional Role of T-Cell Receptor Nanoclusters in Signal Initiation and Antigen Discrimination. *Proc. Natl. Acad. Sci. U.S.A.* **2016**, *113*, E5454–E5463.

(11) Goyette, J.; Nieves, D. J.; Ma, Y.; Gaus, K. How Does T Cell Receptor Clustering Impact on Signal Transduction? *J. Cell Sci.* **2019**, *132*, jcs226423.

(12) Pérez-Ferreros, P.; Gaus, K.; Goyette, J. Tethered Signaling in Inhibitory Immune Receptors. *Front. Phys.* **2019**, *6*, 158.

(13) Adutler-Lieber, S.; Zaretsky, I.; Platzman, I.; Deeg, J.; Friedman, N.; Spatz, J. P.; Geiger, B. Engineering of Synthetic Cellular Microenvironments: Implications for Immunity. *J. Autoimmun.* **2014**, *54*, 100.

(14) Le Saux, G.; Schwartzman, M. Advanced Materials and Devices for the Regulation and Study of NK Cells. *Int. J. Mol. Sci.* **2019**, *20*, 646.

(15) Delcassian, D.; Sattler, S.; Dunlop, I. E. T Cell Immunoengineering with Advanced Biomaterials. *Integr. Biol.* **2017**, *9*, 211–222.

(16) Huang, D.; Patel, K.; Perez-Garrido, S.; Marshall, J. F.; Palma, M. DNA Origami Nanoarrays for Multivalent Investigations of Cancer Cell Spreading with Nanoscale Spatial Resolution and Single-Molecule Control. *ACS Nano* **2019**, *13*, 728–736.

(17) Matic, J.; Deeg, J.; Scheffold, A.; Goldstein, I.; Spatz, J. P. Fine Tuning and Efficient T Cell Activation with Stimulatory ACD3 Nanoarrays. *Nano Lett.* **2013**, *13*, 5090–5097.

(18) Deeg, J.; Axmann, M.; Matic, J.; Liapis, A.; Depoil, D.; Afrose, J.; Curado, S.; Dustin, M. L.; Spatz, J. P. T Cell Activation is Determined by the Number of Presented Antigens. *Nano Lett.* **2013**, *13*, 5619–5626.

(19) Keydar, Y.; Le Saux, G.; Pandey, A.; Avishay, E.; Bar-Hanin, N.; Esti, T.; Bhingardive, V.; Hadad, U.; Porgador, A.; Schwartzman, M. Natural Killer Cells' Immune Response Requires a Minimal Nanoscale Distribution of Activating Antigens. *Nanoscale* **2018**, *10*, 14651–14659.

(20) Cai, H.; Muller, J.; Depoil, D.; Mayya, V.; Sheetz, M. P.; Dustin, M. L.; Wind, S. J. Full Control of Ligand Positioning Reveals Spatial Thresholds for T Cell Receptor Triggering. *Nat. Nanotechnol.* **2018**, *13*, 610–617.

(21) Benard, E.; Nunès, J. A.; Limozin, L.; Sengupta, K. T Cells on Engineered Substrates: The Impact of TCR Clustering Is Enhanced by LFA-1 Engagement. *Front. Immunol.* **2018**, *9*, 2085.

(22) Delcassian, D.; Depoil, D.; Rudnicka, D.; Liu, M.; Davis, D. M.; Dustin, M. L.; Dunlop, I. E. Nanoscale Ligand Spacing Influences Receptor Triggering in T Cells and NK Cells. *Nano Lett.* **2013**, *13*, 5608–5614.

(23) Fang, T.; Alvelid, J.; Spratt, J.; Ambrosetti, E.; Testa, I.; Teixeira, A. I. Spatial Regulation of T-Cell Signaling by Programmed Death-Ligand 1 on Wireframe DNA Origami Flat Sheets. *ACS Nano* **2021**, *15*, 3441–3452.

(24) Hellmeier, J.; Platzer, R.; Eklund, A. S.; Schlichthaerle, T.; Karner, A.; Motsch, V.; Schneider, M. C.; Kurz, E.; Bamieh, V.;

Brameshuber, M.; Preiner, J.; Jungmann, R.; Stockinger, H.; Schütz, G. J.; Huppa, J. B.; Sevcsik, E. DNA Origami Demonstrate the Unique Stimulatory Power of Single PMHCs as T Cell Antigens. *Proc. Natl. Acad. Sci. U.S.A.* **2021**, *118*, No. e2016857118.

(25) Toledo, E.; Le Saux, G.; Edri, A.; Li, L.; Rosenberg, M.; Keidar, Y.; Bhingardive, V.; Radinsky, O.; Hadad, U.; Di Primo, C.; Buffeteau, T.; Smith, A.-S.; Porgador, A.; Schwartzman, M. Molecular-Scale Spatio-Chemical Control of the Activating-Inhibitory Signal Integration in NK Cells. *Sci. Adv.* **2021**, *7*, No. eabc1640.

(26) Trickett, A.; Kwan, Y. L. T cell stimulation and expansion using anti-CD3/CD28 beads. *J. Immunol. Methods* **2003**, *275*, 251–255.

(27) Harris, L. J.; Skaletsky, E.; McPherson, A. Crystallographic structure of an intact IgG1 monoclonal antibody 1 I Edited by I. A. Wilson. *J. Mol. Biol.* **1998**, *275*, 861–872.

(28) Jiménez, D.; Roda-Navarro, P.; Springer, T. A.; Casasnovas, J. M. Contribution of N-Linked Glycans to the Conformation and Function of Intercellular Adhesion Molecules (ICAMs). *J. Biol. Chem.* **2005**, *280*, 5854.

(29) Zak, K. M.; Grudnik, P.; Magiera, K.; Dömling, A.; Dubin, G.; Holak, T. A. Structural Biology of the Immune Checkpoint Receptor PD-1 and Its Ligands PD-L1/PD-L2. *Structure* **2017**, *25*, 1163–1174.

(30) Le Saux, G.; Edri, A.; Keydar, Y.; Hadad, U.; Porgador, A.; Schwartzman, M. Spatial and Chemical Surface Guidance of NK Cell Cytotoxic Activity. *ACS Appl. Mater. Interfaces* **2018**, *10*, 11486–11494.

(31) Odom, T. W.; Love, J. C.; Wolfe, D. B.; Paul, K. E.; Whitesides, G. M. Improved Pattern Transfer in Soft Lithography Using Composite Stamps. *Langmuir* **2002**, *18*, 5314–5320.

(32) Pandey, A.; Tzadka, S.; Yehuda, D.; Schwartzman, M. Soft Thermal Nanoimprint with a 10 Nm Feature Size. *Soft Matter* **2019**, *15*, 2897.

(33) Krzewski, K.; Gil-Krzewska, A.; Nguyen, V.; Peruzzi, G.; Coligan, J. E. LAMP1/CD107a Is Required for Efficient Perforin Delivery to Lytic Granules and NK-Cell Cytotoxicity. *Blood* **2013**, *121*, 4672–4683.

(34) Bertrand, F.; Muller, S.; Roh, K.-H.; Laurent, C.; Dupre, L.; Valitutti, S. An Initial and Rapid Step of Lytic Granule Secretion Precedes Microtubule Organizing Center Polarization at the Cytotoxic T Lymphocyte/Target Cell Synapse. *Proc. Natl. Acad. Sci. U.S.A.* **2013**, *110*, 6073–6078.

(35) Aktas, E.; Kucuksezer, U. C.; Bilgic, S.; Erten, G.; Deniz, G. Relationship between CD107a Expression and Cytotoxic Activity. *Cell. Immunol.* **2009**, *254*, 149–154.

(36) Bhat, P.; Leggatt, G.; Waterhouse, N.; Frazer, I. H. Interferon- γ Derived from Cytotoxic Lymphocytes Directly Enhances Their Motility and Cytotoxicity. *Cell Death Dis.* **2017**, *8*, No. e2836.

(37) Guasch, J.; Conings, B.; Neubauer, S.; Rechenmacher, F.; Ende, K.; Rolli, C. G.; Kappel, C.; Schaufler, V.; Micoulet, A.; Kessler, H.; Boyen, H.-G.; Cavalcanti-Adam, E. A.; Spatz, J. P. Segregation Versus Colocalization: Orthogonally Functionalized Binary Micropatterned Substrates Regulate the Molecular Distribution in Focal Adhesions. *Adv. Mater.* **2015**, *27*, 3737–3747.

(38) Le Saux, G.; Wu, M. C.; Toledo, E.; Chen, Y. Q.; Fan, Y. J.; Kuo, J. C.; Schwartzman, M. Cell-Cell Adhesion-Driven Contact Guidance and Its Effect on Human Mesenchymal Stem Cell Differentiation. *ACS Appl. Mater. Interfaces* **2020**, *12*, 22399–22409.

(39) Doh, J.; Irvine, D. J. Immunological Synapse Arrays: Patterned Protein Surfaces That Modulate Immunological Synapse Structure Formation in T Cells. *Proc. Natl. Acad. Sci. U.S.A.* **2006**, *103*, 5700–5705.

(40) Culley, F. J.; Johnson, M.; Evans, J. H.; Kumar, S.; Crilly, R.; Casasbuenas, J.; Schnyder, T.; Mehrabi, M.; Deonarain, M. P.; Ushakov, D. S.; Braud, V.; Roth, G.; Brock, R.; Köhler, K.; Davis, D. M. Natural Killer Cell Signal Integration Balances Synapse Symmetry and Migration. *PLoS Biol.* **2009**, *7*, No. e1000159.